

# Quantification of the $\pi$ – $\pi$ Interactions that Govern Tertiary Structure in Donor–Acceptor [2]Pseudorotaxanes

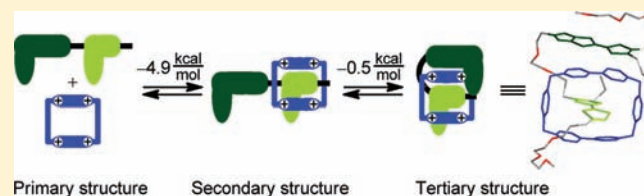
Stinne W. Hansen,<sup>†,‡</sup> Paul C. Stein,<sup>†</sup> Anne Sørensen,<sup>†</sup> Andrew I. Share,<sup>‡</sup> Edward H. Witlicki,<sup>‡</sup> Jacob Kongsted,<sup>†</sup> Amar H. Flood,<sup>‡</sup> and Jan O. Jeppesen<sup>\*,†</sup>

<sup>†</sup>Department of Physics, Chemistry, and Pharmacy, University of Southern Denmark, Campusvej 55, 5230 Odense M, Denmark

<sup>‡</sup>Department of Chemistry, Indiana University, 800 East Kirkwood Avenue, Bloomington, Indiana 47405, United States

## Supporting Information

**ABSTRACT:** Flexibility in pseudorotaxanes and interlocked molecules that rely on interactions between  $\pi$ –donor–acceptor subunits provides access to folded structures reminiscent of the tertiary structure of proteins. While they have been described before, only now have we been able to quantify one such tertiary structure by making use of pseudorotaxanes designed for the purpose. Here, the enhanced stability of a pseudorotaxane inside a folded structure is measured to be  $\Delta G = \text{ca. } 0.5 \text{ kcal mol}^{-1}$ . The tertiary structure is stabilized by a charge-transfer interaction between a tetrathiafulvalene-based  $\pi$ -donor that can situate alongside a  $\pi$ -accepting paraquat-based macrocycle by folding of a flexible linker. At room temperature, it was estimated that 70% of the pseudorotaxanes examined here exist in their folded state. This quantitative information is critical for the creation of interlocked molecular machines that have predictable energetics and structures and for revealing a complexity approaching biological molecules.



## INTRODUCTION

The field of supramolecular chemistry was initiated approximately 40 years ago and is today a vibrant area of contemporary research<sup>1</sup> that has recently branched out into nanoscience.<sup>2–4</sup> Supramolecular systems rely on weak non-covalent interactions such as hydrogen bonding,  $\pi$ – $\pi$  interactions, and donor–acceptor interactions and exploit naturally occurring phenomena like self-organization, self-assembly, self-replication, and molecular recognition. The remarkable properties of proteins and DNA are only possible because the same noncovalent interactions that control their folding and assembly are sufficient to overcome conformational chaos. In addition to sharing these phenomena and interactions, nature also serves as an inexhaustible source of inspiration and analogy in supramolecular science. Here, we apply the concepts of a protein's primary (1°), secondary (2°), and tertiary (3°) structure (Figure 1) to the emergence of ordered structures in pseudorotaxanes as a means to help understand the energetics of folded states that have hitherto been inaccessible despite being spotted in a few instances.<sup>5</sup>

The focus on pseudorotaxanes is based on their ability to forecast rotaxanes, which are interlocked molecules with “rod-in-ring” rotaxanes, capable of performing molecular motions<sup>6</sup> and acting as nanoscale machinery. Success with this functional outcome has almost always relied upon the selection and sequence of stations along the rod (1° structure, Figure 1) to generate a predictable 2° structure where the localization of the ring at one station over another is determined by well-known noncovalent bonds. The 3° structures, however, have usually been overlooked presumably because they are difficult to

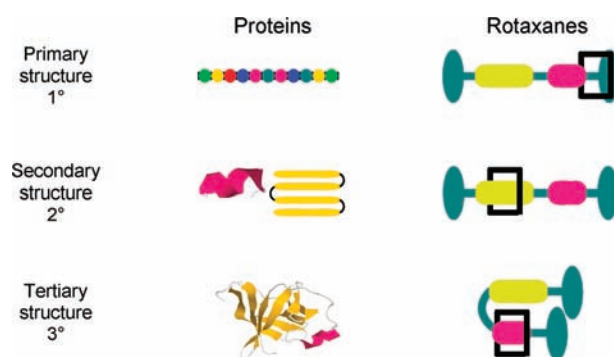


**Figure 1.** Hierarchical organization of protein structure serves as an analogy for threaded complexes and interlocked molecules. The 3° protein structure shown is the crystal structure of human recombinant MTCP-1.<sup>8</sup>

observe. Yet, the folded states can cause the properties of molecular machines to diverge from predictions when they are based solely on 1° and 2° design considerations. For example, a bistable rotaxane unexpectedly lost ca. 50% of its switchable character.<sup>5a</sup> This outcome was believed to arise from a folded state; a 3° structure that was later supported qualitatively.<sup>5b</sup> Thus, when the same depth of understanding that is enjoyed in the creation of 2° structures is extended to the 3° level,<sup>7</sup> both

Received: November 18, 2011

Published: January 17, 2012

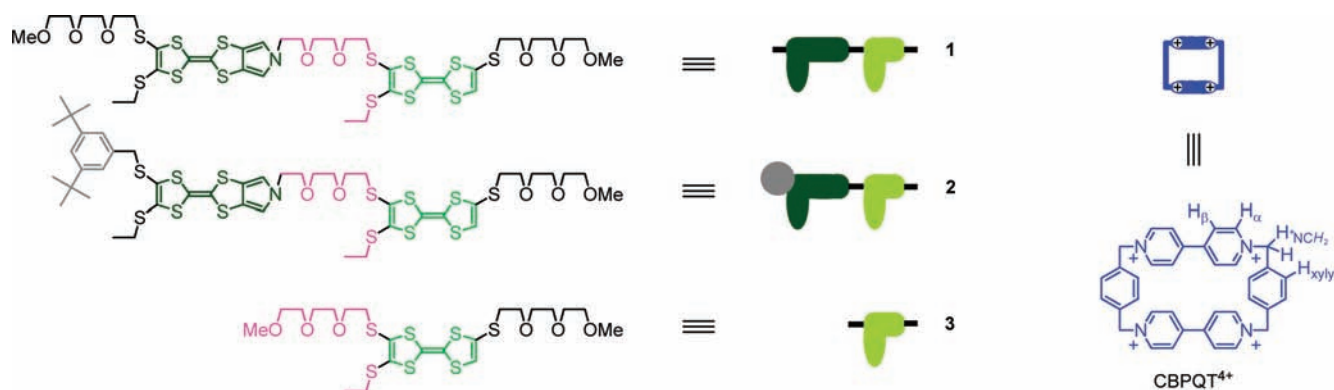


**Figure 2.** Molecular structures of the semidumbbells 1–3 and  $\text{CBPQT}^{4+}$  and their corresponding cartoon representations.

the accuracy of our designs and opportunities for new ones can grow.

Studies identifying  $3^\circ$  structures in interlocked molecules are small in number. It is the flexible poly(ethyleneglycol) (PEG) linkers present in the majority of rotaxanes containing  $\pi$ -electron rich stations that allow the folded  $3^\circ$  structure to exist. There has been early focus on the C–H $\cdots$ O hydrogen bonding between the cyclobis(paraquat-*p*-phenylene)<sup>9</sup> ( $\text{CBPQT}^{4+}$ )  $\alpha$ -protons and the PEG linker oxygens,<sup>2d,10</sup> taking place on the exterior of the complex. However, what has emerged in recent works<sup>5a,b</sup> is the need to deliver a quantitative account of the charge–transfer (CT) interactions that help determine the folded  $3^\circ$  structure—in addition to the C–H $\cdots$ O hydrogen bonds. These CT interactions are prevalent, if not universal, when  $\pi$ -derived donors and acceptors are used in redox-active molecular machines for demonstrations of molecular electronics,<sup>2</sup> molecular muscles,<sup>3</sup> and RGB electrochromic materials<sup>4</sup> that highlight the potential of interlocked molecules in nanotechnology.

In this work, we present the synthesis and investigation of foldable [2]pseudorotaxanes based on  $\text{CBPQT}^{4+}$  and semidumbbells (1 or 2, Figure 2) incorporating two different tetrathiafulvalene<sup>11</sup> (TTF) units. These designs render it possible to investigate and quantify the CT interactions that govern the  $3^\circ$  alongside structure in  $\pi$ -donor–acceptor [2]pseudorotaxanes.

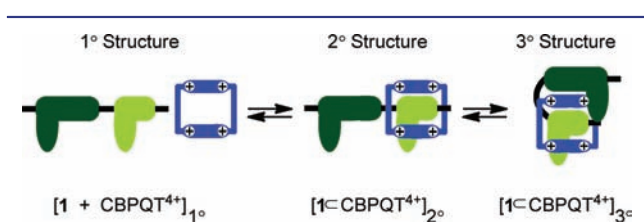


**Figure 3.** Representations of the complexation and folding equilibria between the semidumbbell 1 and  $\text{CBPQT}^{4+}$  (blue) show different levels of structural organization. After complexation of  $\text{CBPQT}^{4+}$  with TTF (light green), the MPTTF unit (dark green) can fold back and interact with  $\text{CBPQT}^{4+}$  in an alongside manner stabilized by CT interactions.

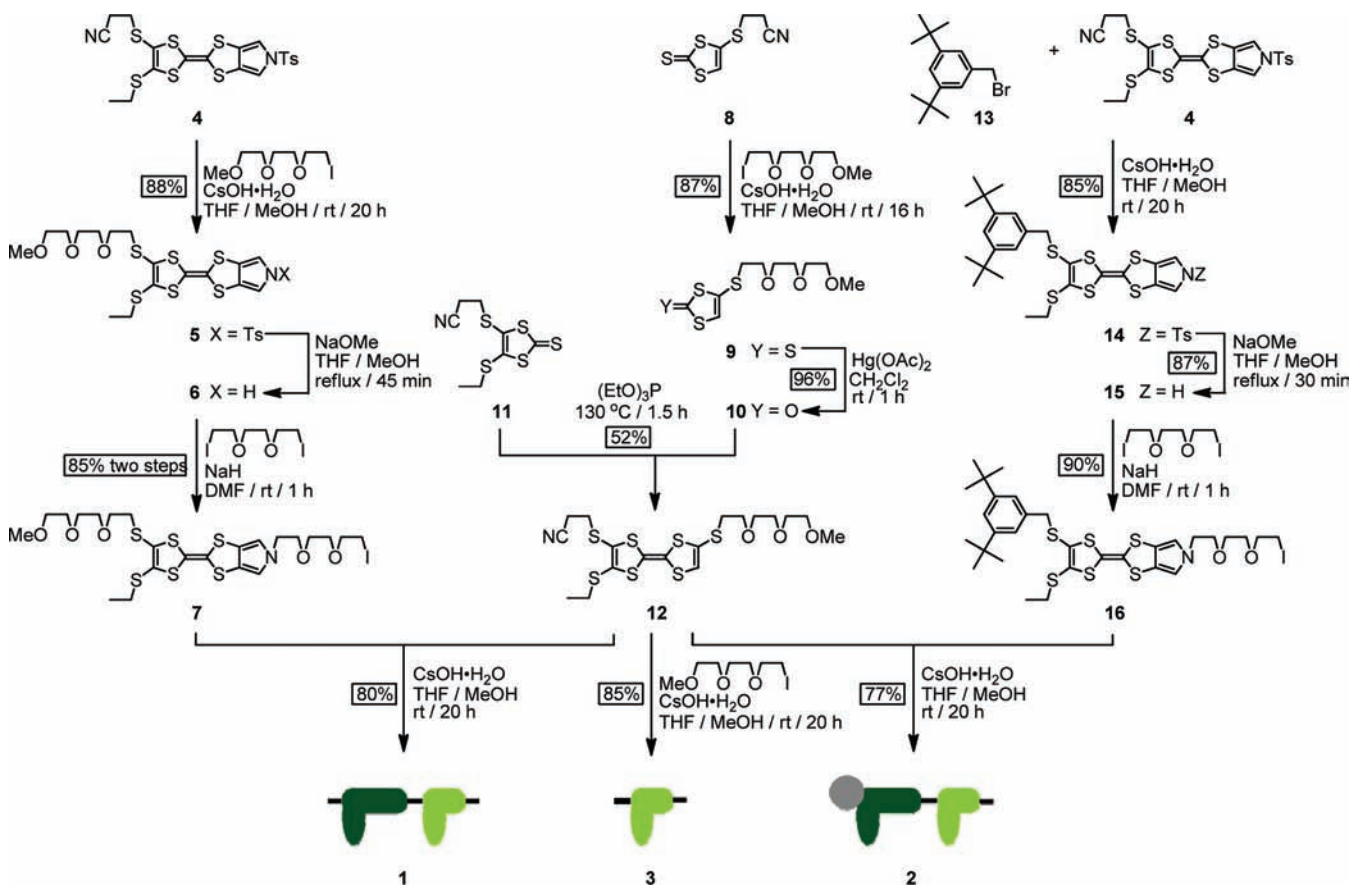
The  $1^\circ$  structures of all the semidumbbells (Figures 2 and 3) are designed to be nonsymmetric along the east–west axis. The entire west side is a stopper with internal structure, whereas the east side is the binding site. Consequently, the  $\text{CBPQT}^{4+}$  ring can only access the TTF unit (light green) by threading over the triethylene glycol (TEG) linker on the east side of 1 and 2.

In the  $2^\circ$  structure of the complex, the  $\text{CBPQT}^{4+}$  ring is restricted to encircle the TTF unit (Figure 3,  $[\text{1-CBPQT}^{4+}]_{2^\circ}$ ) since the combination of the SEt group (purple) and the central thioglycol linker (purple) provide a kinetic barrier, i.e., they act together as a stopper. The thioglycol linker was introduced to provide the flexibility necessary to allow the monopyrroloTTF<sup>12</sup> (MPTTF) unit within the stopper on the west side to fold back onto the  $\text{CBPQT}^{4+}$  ring. In this way, it can interact in an alongside manner generating a  $3^\circ$  structure (Figure 3,  $[\text{1-CBPQT}^{4+}]_{3^\circ}$ ). Semidumbbell 3 has been designed to consist solely of a TTF unit similar to the east side of semidumbbells 1 and 2. It is assumed that the TTF unit of semidumbbell 3 will have the same binding energy with the  $\text{CBPQT}^{4+}$  ring as the east sides of semidumbbells 1 and 2. This assumption makes it possible to quantify the additional binding energy provided by the folding of the supermolecule into a  $3^\circ$  structure stabilized by CT interactions with the west side MPTTF unit and the exterior of the  $\text{CBPQT}^{4+}$  ring. The semidumbbells 1–3 all exist as two different isomers on account of the inherent *E/Z* isomerism of the TTF unit. Since the ratios of the isomers are all the same, this is thought to be of minor importance.

## RESULTS AND DISCUSSION

**Synthesis.** The semidumbbells 1–3 were synthesized (Scheme 1) using a convergent synthetic strategy. The MPTTF building block<sup>2d</sup> 4 was alkylated with 1-iodo-2-[2-(2-methoxyethoxy)ethoxy]ethane<sup>13</sup> following its in situ deprotection with  $\text{CsOH}\cdot\text{H}_2\text{O}$  to give MPTTF 5 in 88% yield. The tosyl protecting group was removed by NaOMe in a THF/MeOH mixture and the resulting free pyrrole nitrogen in compound 6 was *N*-alkylated (NaH/DMF) with 1,2-bis(2-iodoethoxy)ethane,<sup>14</sup> affording the MPTTF building block 7 in 85% yield over two steps. The thione<sup>15</sup> 8 was *S*-alkylated with 1-iodo-2-[2-(2-methoxyethoxy)ethoxy]ethane after in situ deprotection with  $\text{CsOH}\cdot\text{H}_2\text{O}$  in 87% yield to afford the thione 9 which was transchalcogenated using  $\text{Hg}(\text{OAc})_2$  in  $\text{CH}_2\text{Cl}_2$  to the corresponding ketone 10 in 96% yield. The ketone 10 was cross coupled with the thione<sup>16</sup> 11 yielding the TTF building block 12 in 52% yield. This building block was in situ deprotected with  $\text{CsOH}\cdot\text{H}_2\text{O}$  and afterward *S*-alkylated in THF/MeOH with either 1-iodo-2-[2-(2-methoxyethoxy)ethoxy]ethane to give semidumbbell 3 in 85% yield or with the MPTTF building block 7 giving semidumbbell 1 in 80% yield. Semidumbbell 2 was also prepared from the MPTTF building block 4 and 3,5-di-*tert*-butylbenzylbromide<sup>17</sup> 13 in a series of reactions identical to those used for the synthesis of 2

Scheme 1. Synthesis of the Semi-Dumbbells 1–3



and in comparable yields (Scheme 1). All of the compounds containing the TTF unit were isolated as mixtures of *E/Z* isomers and  $^1\text{H}$  NMR spectroscopy confirmed (Supporting Information) that the ratio between the isomers was 1:1 in all cases.

**Binding Constant Determinations.** Comparisons of the binding between the  $\text{CBPQT}^{4+}$  ring and semidumbbells 1–3 indicate that the presence of the alongside interaction affords a  $0.5 \text{ kcal mol}^{-1}$  boost to the free energy of binding. The individual binding constants were characterized (Figure 4) by

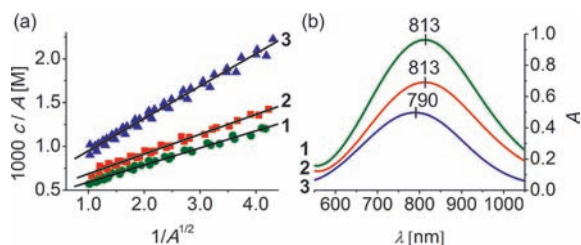


**Figure 4.** (a) Plots of  $c/A$  against  $1/A^{1/2}$  for 1:1 mixtures of  $\text{CBPQT}^{4+}$  and the semidumbbells 1–3. The absorbance ( $A$ ) was measured at several different absolute concentrations ( $c$ ) obtained from dilution of at least two independent stock solutions in MeCN at 298 K. (b) A comparison of the CT bands for 1:1 mixtures of  $\text{CBPQT}^{4+}$  and the semidumbbells 1–3 at the conditions  $0.5 \text{ mM} + 1 \text{ equiv CBPQT}^{4+}$ .

absorption spectroscopy using the dilution method.<sup>10c,18</sup> Mixing equimolar amounts of the  $\text{CBPQT}^{4+}$  ring and each of the semidumbbells 1–3 in MeCN results in the formation of the corresponding [2]pseudorotaxanes confirmed by the

immediate color change of the solution from yellow to green and the concomitant appearance of CT bands in the 790–813 nm region of the absorption spectra. The  $K_a$  values were determined from the linear plots of  $c/A$  against  $1/A^{1/2}$  (Figure 4a) for 1:1 mixtures of  $\text{CBPQT}^{4+}$  and the semidumbbells 1–3 (Supporting Information) at 298 K in MeCN and the data obtained are summarized in Table 1. The binding constants

**Table 1. Comparison of Binding Constants, Extinction Coefficients, and Derived Free Energies of Complexation between  $\text{CBPQT}^{4+}$  and the Semi-Dumbbells 1–3<sup>a</sup>**

complex	$K_a$ [ $\text{M}^{-1}$ ]	$\epsilon$ [ $\text{M}^{-1} \text{ cm}^{-1}$ ]	$\Delta G^\circ$ [ $\text{kcal mol}^{-1}$ ]
1 C $\text{CBPQT}^{4+}$	$10300 \pm 1400$	$2500 \pm 600$	$-5.5 \pm 0.1$
2 C $\text{CBPQT}^{4+}$	$9000 \pm 1500$	$2200 \pm 500$	$-5.4 \pm 0.1$
3 C $\text{CBPQT}^{4+}$	$4200 \pm 600$	$1700 \pm 500$	$-4.9 \pm 0.1$

<sup>a</sup>Determined by absorption spectroscopy at 298 K in MeCN using the NIR CT band as probe. The errors were obtained as described by Nygaard et al.

( $K_a$ ) for the semidumbbells 1 and 2 are more than twice as large as 3. This finding indicates that the presence of the MPTTF unit results in a stabilizing effect of approximately  $0.5 \text{ kcal mol}^{-1}$  on the complex formed between  $\text{CBPQT}^{4+}$  and the TTF unit. We ascribe this to a folded 3° structure (Figure 3) stabilized by CT interactions taking place between the MPTTF unit and one of the bipyridinium moieties of  $\text{CBPQT}^{4+}$ . Consistently, the extinction coefficients (Table 1) of the CT electronic transitions generated (Supporting Information) in the fitting analysis are greater for both 1 and 2 when compared to 3, and the bandwidths are larger (Figure 4b). The additional

CT interaction is expected to be accompanied by another electronic transition that, based on prior work,<sup>19</sup> is likely to be situated at another location. Therefore, both factors would lead to the enhanced and broadened band in the NIR region.

The  $K_a$  values for pseudorotaxanes  $1\text{CCBPQT}^{4+}$  and  $2\text{CCBPQT}^{4+}$  are the same to within error. This outcome was not predictable on the basis of the structures (Figure 2). The TEG substituent on the far west side of MPTTF unit in semidumbbell **1** has the possibility of forming hydrogen bonding interactions between the acidic  $\alpha$ -CH protons in the bipyridinium moieties of  $\text{CBPQT}^{4+}$  and some of the oxygen atoms in the TEG chain.<sup>10c</sup> These interactions would be absent in semidumbbell **2**. Thus, the equivalence of the binding affinities indicate that neither the potentially “sticky” TEG nor the “bulky” stopper groups, which are located beyond the MPTTF unit folded onto the side of the  $\text{CBPQT}^{4+}$  ring do not have a major impact on the stability of the  $3^\circ$  structure.

**Molecular Modeling.** In order to get a better understanding of the nature of the binding interactions present in the two [2]pseudorotaxanes  $1\text{CCBPQT}^{4+}$  and  $2\text{CCBPQT}^{4+}$ , density functional theory has been employed with the M06-L exchange-correlation functional,<sup>20</sup> implemented in Jaguar 7.6,<sup>21</sup> to provide a quantum mechanically based description of the geometry of the  $3^\circ$  superstructures. This exchange-correlation functional has previously been used to provide accurate structural and energetic descriptions of superstructures and mechanically interlocked molecules.<sup>22</sup> We have performed geometry optimizations for the pseudorotaxanes with  $\text{CBPQT}^{4+}$  encircling the TTF unit of semidumbbells **1** and **2** at the M06-L/6-31G\*\* level of theory including solvent corrections in MeCN ( $\epsilon = 37.5$ ,  $R_0 = 2.18 \text{ \AA}$ ) based on the Poisson–Boltzmann dielectric continuum model implemented in Jaguar.

In the optimized structures (Figure 5),  $\text{CBPQT}^{4+}$  encircles the TTF unit with TTF...bipyridinium distances of  $3.5 \text{ \AA}$  in

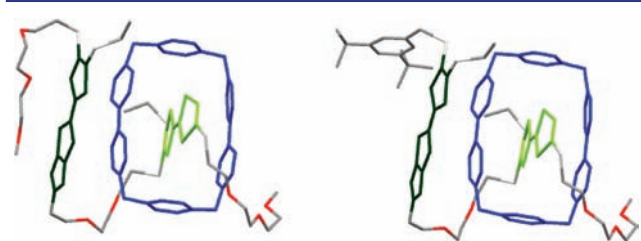


**Figure 5.** M06-L/6-31G\*\* geometry optimized superstructures (solvent corrected, MeCN) of the two [2]pseudorotaxanes  $[1\text{CCBPQT}^{4+}]_3^\circ$  (left) and  $[2\text{CCBPQT}^{4+}]_3^\circ$  (right). For clarity no hydrogens are shown and the TTF unit is colored light green, MPTTF dark green,  $\text{CBPQT}^{4+}$  blue, other atoms: carbon = dark gray, sulfur = light gray and oxygen = red.

agreement<sup>23</sup> with the optimal distance for donor–acceptor interactions. The MPTTF unit is engaged in an alongside CT interaction with one of the bipyridinium moieties in  $\text{CBPQT}^{4+}$  with a MPTTF...bipyridinium distance of  $3.5 \text{ \AA}$ . Consistent with the enhanced stability and UV–vis–NIR absorption properties, these ground state CT interactions are furthermore theoretically supported by natural population analysis. When conducted at the same level as described above they reveal that the charge of  $\text{CBPQT}^{4+}$  is reduced by 0.85 and 0.92 atomic units (au) in  $[1\text{CCBPQT}^{4+}]_3^\circ$  and  $[2\text{CCBPQT}^{4+}]_3^\circ$ , respectively, upon complexation. Furthermore, for both complexes 0.43 au of the transferred charge is found to originate from the

MPTTF unit of either **1** or **2** indicating that an alongside CT interaction can exist. In addition, the optimized structures show geometries consistent with hydrogen bonding interactions taking place between one of the  $\text{CBPQT}^{4+}$  pyridinium  $\alpha$ -protons and TEG oxygens (ca.  $2.5 \text{ \AA}$ ) with the glycol linkers on either side of the TTF unit. However, the glycol chain on MPTTF in the semidumbbell **1** folds back on itself neither favoring nor disfavoring the folded  $3^\circ$  structure. The bulky di-*tert*-butylbenzylic stopper from semidumbbell **2** also folds away from the  $\text{CBPQT}^{4+}$  ring, and therefore it will not sterically disfavor the folded  $3^\circ$  structure.

These findings are in complete agreement with the results obtained from the solution-phase binding studies showing a negligible difference in the binding constants (Table 1) between the  $\text{CBPQT}^{4+}$  and the semidumbbells **1** and **2**, respectively. That is, the MPTTF unit seems to contribute the same degree of extra stabilization to the [2]pseudorotaxanes  $1\text{CCBPQT}^{4+}$  and  $2\text{CCBPQT}^{4+}$ , regardless of substitution on the MPTTF unit with either the TEG or bulky di-*tert*-butylbenzylic stopper.

**$^1\text{H}$  NMR Spectroscopy.** The complexation between the  $\text{CBPQT}^{4+}$  ring and semidumbbells **1** and **3** and the subsequent folding in  $1\text{CCBPQT}^{4+}$  have been studied by variable temperature (VT) and two-dimensional (2D)  $^1\text{H}$  NMR spectroscopy. Complete assignments of the  $^1\text{H}$  NMR spectra are complicated by the need to count for 87 and 68 protons present in  $1\text{CCBPQT}^{4+}$  and  $3\text{CCBPQT}^{4+}$ , respectively, together with the fact that both complexes are in equilibrium with their free constituents and the semidumbbells exist as two *E/Z* isomers.

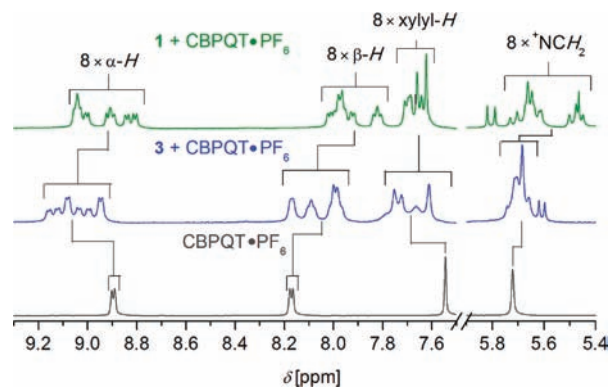


**Figure 6.** Partial  $^1\text{H}$  NMR spectra (500 MHz, 233 K,  $\text{CD}_3\text{CN}$ ) of: top, green: semidumbbell **1** + 0.75 equiv.  $\text{CBPQT}\cdot 4\text{PF}_6$ , middle, blue: semidumbbell **3** + 0.75 equiv.  $\text{CBPQT}\cdot 4\text{PF}_6$ , bottom, gray:  $\text{CBPQT}\cdot 4\text{PF}_6$ .

In the case of the complex formed between the semidumbbell **3** and  $\text{CBPQT}^{4+}$ , exchange between the complexed and uncomplexed species occurs rapidly (Supporting Information, Figure S5) on the  $^1\text{H}$  NMR time scale ( $\text{CD}_3\text{CN}$ , 500 MHz) at 293 K. Decreasing the temperature of the  $\text{CD}_3\text{CN}$  sample favors complexation, and at 233 K, the kinetics is in the regime of slow exchange, and both complexed and uncomplexed semidumbbell can be observed (Figure S4 of the SI) in the  $^1\text{H}$  NMR spectrum recorded of **3** and 0.75 equivalents of  $\text{CBPQT}^{4+}$ . However, no signals associated with uncomplexed  $\text{CBPQT}^{4+}$  are present (Figure 6) in the  $^1\text{H}$  NMR spectrum indicating that the complexation is very strong at 233 K. A close examination of the  $^1\text{H}$  COSY (correlation spectroscopy)

spectrum (Figure S7 of the SI) reveals that eight doublets ( $J = 6.5$  Hz) are present between 8.93 and 9.15 ppm and eight doublets ( $J = 6.5$  Hz) are present between 7.96 and 8.17 ppm. It is well-known<sup>4b,5c,18,24</sup> that signals in these regions for these particular types of complexes can be associated with the resonances for the bipyridinium  $H_\alpha$  and  $H_\beta$  protons (Figure 2), respectively. The presence of eight  $H_\alpha$  and  $H_\beta$  resonances confirms that  $3\text{CCBPQT}^{4+}$  exists as a mixture of  $E/Z$  isomers. On account of the low degree of symmetry of the semidumbbell **3** and the lack of free rotation in the  $\text{CBPQT}^{4+}$  ring at 233 K, desymmetrization of the complexed  $\text{CBPQT}^{4+}$  ring will take place and four signals<sup>5b,25</sup> of  $H_\alpha$  and  $H_\beta$  will appear for both the  $E$  and the  $Z$  isomer. These effects were also seen when studying the complexation between **1** and  $\text{CBPQT}^{4+}$  but with one noteworthy difference. Even though the cyclophane in  $1\text{CCBPQT}^{4+}$  resides on a TTF unit that is identical to the one in **3**, the resonances of the cyclophane  $H_\alpha$  and  $H_\beta$  protons are shifted upfield in comparison to  $3\text{CCBPQT}^{4+}$ . This upfield shift is indicative<sup>5c</sup> of  $\pi$ - $\pi$  interactions and is assigned to stacking between one of bipyridinium moieties of  $\text{CBPQT}^{4+}$  and the MPTTF unit residing alongside it in the folded  $3^\circ$  structure (Figure 3). The upfield shift is consistent with increased shielding effect of the protons in the  $\text{CBPQT}^{4+}$  ring. The effect is also evident in some of the  $^1\text{NCH}_2$  protons of the  $\text{CBPQT}^{4+}$  ring (Figure 6), but less so in the positions of the  $p$ -xylyl protons as they are not directly engaged in the structure-determining  $\pi$ - $\pi$  interactions.

NOESY experiments were also carried out in  $\text{CD}_3\text{CN}$  at 233 K and in  $\text{CD}_3\text{COCD}_3$  at 203 K. However, it was not possible to observe any NOE effect between the protons in MPTTF unit and the protons on the  $\text{CBPQT}^{4+}$  ring, which most likely can be accounted for by the dynamic nature of the complex even at low temperatures.<sup>26</sup>

**Electrochemical Investigations.** With strong evidence for the folded  $3^\circ$  structures available, cyclic voltammetry (CV) was used to probe the changes in the redox potentials of the semidumbbell **1** when the alongside CT interaction is in place. The first oxidation process of the free semidumbbell **1** (Figure 7, black trace) appears at  $E_{1/2}^1 = +0.39$  V and is associated with

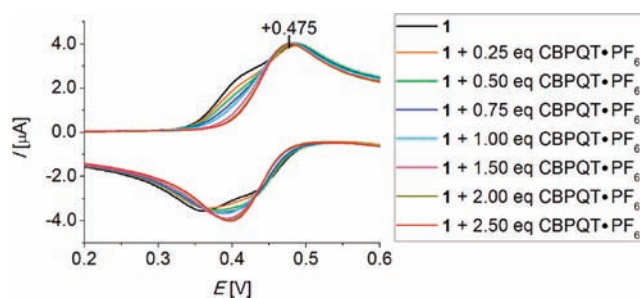


**Figure 7.** Partial cyclic voltammograms of a titration of the semidumbbell **1** with 0–2.50 equiv. of  $\text{CBPQT}\cdot\text{PF}_6$ . CV measurements were carried out at 265 K in argon-purged MeCN solutions (1.0 mM) with tetrabutylammonium hexafluorophosphate ( $n\text{-Bu}_4\text{NPF}_6$ ) as supporting electrolyte (0.1 M) and glassy carbon as working electrode, platinum wire as auxiliary electrode at a scan rate of  $200\text{ mV s}^{-1}$ . Potential values in V vs  $\text{Ag}/\text{AgCl}$ .

oxidation of the MPTTF unit (Supporting Information), whereas the second oxidation process appearing at  $E_{1/2}^2 = +0.46$  V is assigned to the oxidation of the TTF unit (Supporting Information) and both generate monocations. Upon addition of increasing amounts of  $\text{CBPQT}^{4+}$  to the

solution, the first oxidation process associated with the MPTTF unit shifts anodically by +75 mV to +0.475 V. Therefore, the peak observed at +0.475 V can be assigned to two different overlapping oxidation processes. The oxidation of the MPTTF unit shifts in a manner consistent with the alongside interaction with  $\text{CBPQT}^{4+}$ ; MPTTF units become more difficult to oxidize when engaged in a CT interaction.<sup>23b</sup> The first oxidation of the TTF unit, now encircled by  $\text{CBPQT}^{4+}$ , also occurs at +0.475 V. Such a change was also seen (Supporting Information) when  $\text{CBPQT}^{4+}$  was titrated into the semidumbbell **3**. These changes are subtle, highlighting how easy they are to overlook in two-station pseudototaxanes<sup>5b</sup> and rotaxanes<sup>5a</sup> based on TTF units.

**Resonance Raman Spectroscopy.** The  $1\text{CCBPQT}^{4+}$  pseudorotaxane was studied by resonance Raman spectroscopy to inspect for signatures of the alongside interaction; as has been previously observed.<sup>19</sup> On the basis of the broadened CT bands (Figure 4b), it was hoped that MPTTF vibrations would be enhanced at different locations to TTF. Unfortunately, it was not possible to detect the alongside interaction by that technique presumably because the  $\text{MPTTF} \rightarrow \text{CBPQT}^{4+}$  transition was too weak and/or its Raman bands coincided with the  $\text{TTF} \rightarrow \text{CBPQT}^{4+}$  transition.

## CONCLUSIONS

The alongside  $\pi$ - $\pi$  interactions observed in rotaxanes with more than one  $\pi$ -electron donor were seen here in numerous forms: chemical shift changes, altered redox properties, enhanced binding affinities, modified absorption band intensities, and band widths, as well as supporting computer-generated structures. By absorption spectroscopic investigations, it has been possible, for the first time, to quantify the  $\pi$ - $\pi$  interactions. The binding studies carried out on  $1$ – $3\text{CCBPQT}^{4+}$  revealed that the complexation ability of  $\text{CBPQT}^{4+}$  with semidumbbells **1** and **2** is  $0.5 \pm 0.2$  kcal  $\text{mol}^{-1}$  higher as compared to the model compound **3**. Assuming that the relative distribution between the  $2^\circ$  and  $3^\circ$  structures is related to this free energy difference, it can be calculated<sup>27</sup> that the equilibrium constant ( $K_{\text{eq}}$ ) between the unfolded  $2^\circ$  structure and the folded  $3^\circ$  structure is  $2.3 \pm 0.8$ . This  $K_{\text{eq}}$  value implies that approximately 70% of  $1\text{CCBPQT}^{4+}$  and  $2\text{CCBPQT}^{4+}$  exists (Figure 8) in their folded  $3^\circ$  structures in MeCN at 298 K.

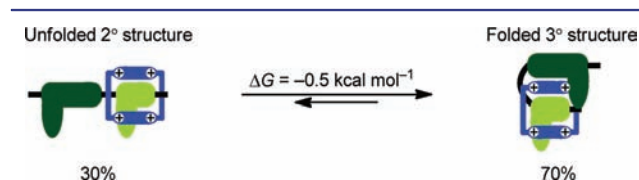


**Figure 8.** The equilibrium between the  $2^\circ$  and  $3^\circ$  structures is shifted toward the folded  $3^\circ$  structure on account of the stabilizing effect of  $0.5$  kcal  $\text{mol}^{-1}$  from the  $\pi$ - $\pi$  interactions between the bipyridinium moieties of  $\text{CBPQT}^{4+}$  (blue) and the MPTTF unit (dark green).

An extra stabilization of the pseudorotaxanes by  $0.5$  kcal  $\text{mol}^{-1}$  is a reasonable adjustment to include in designs of bistable [2]rotaxanes. While small, the 2-fold enhancement in the binding affinity can become significant, particularly when it is structure-determining; taking a rotaxane and folding it back upon itself. The impact of this interaction on the tertiary structure must also be accounted for in the designed functionality of molecular machines just as nature accommodates and uses them in the performance of biomachines.

## ■ ASSOCIATED CONTENT

## ■ Supporting Information

Experimental procedures for synthesis of the semidumbbells 1–3, description of binding studies, XYZ coordinates for calculated super structures, variable temperature <sup>1</sup>H NMR studies, and description of electrochemical measurements. This material is available free of charge via the Internet at <http://pubs.acs.org>.

## ■ AUTHOR INFORMATION

## Corresponding Author

joj@ifk.sdu.dk.

## Notes

The authors declare no competing financial interest.

## ■ ACKNOWLEDGMENTS

This work was supported by the Center for Fundamental Living Technology (FLinT), University of Southern Denmark (SDU), the Villum Foundation, and The Danish Natural Science Research Council (FNU, projects no. 272-08-0578). A.H.F. thanks the Dreyfus Foundation for support.

## ■ REFERENCES

- (1) (a) Lehn, J.-M. *Supramolecular Chemistry*; 1. ed.; Wiley-VCH: Weinheim, Germany, 1995. (b) Whitesides, G. M.; Grzybowski, B. *Science* **2002**, *295*, 2418–2421. (c) Stoddart, J. F. *Nat. Chem.* **2009**, *1*, 14–15.
- (2) (a) Collier, C. P.; Mattersteig, G.; Wong, E. W.; Luo, Y.; Beverly, K.; Sampaio, J.; Raymo, F. H.; Stoddart, J. F.; Heath, J. R. *Science* **2000**, *289*, 1172–1175. (b) Luo, Y.; Collier, C. P.; Jeppesen, J. O.; Nielsen, K. A.; DeIonno, E.; Ho, G.; Perkins, J.; Tseng, H.-R.; Yamamoto, T.; Stoddart, J. F.; Heath, J. R. *ChemPhysChem* **2002**, *3*, 519–525. (c) Steuerman, D. W.; Tseng, H.-R.; Peters, A. J.; Flood, A. H.; Jeppesen, J. O.; Nielsen, K. A.; Stoddart, J. F.; Heath, J. R. *Angew. Chem., Int. Ed.* **2004**, *43*, 6486–6491. (d) Choi, J. W.; Flood, A. H.; Steuerman, D. W.; Nygaard, S.; Braunschweig, A. B.; Moonen, N. N. P.; Laursen, B. W.; Luo, Y.; DeIonno, E.; Peters, A. J.; Jeppesen, J. O.; Xu, K.; Stoddart, J. F.; Heath, J. R. *Chem.—Eur. J.* **2006**, *12*, 261–279. (e) Zhang, W.; DeIonno, E.; Dichtel, W. R.; Fang, L.; Trabolsi, A.; Olsen, J.-C.; Benitez, D.; Heath, J. R.; Stoddart, J. F. *J. Mater. Chem.* **2011**, *21*, 1487–1495.
- (3) (a) Jimenez-Molero, M. C.; Dietrich-Buchecker, C.; Sauvage, J. P. *Chem.—Eur. J.* **2002**, *8*, 1456–1466. (b) Liu, Y.; et al. *J. Am. Chem. Soc.* **2005**, *127*, 9745–9759. (c) Juluri, B. K.; Kumar, A. S.; Liu, Y.; Ye, T.; Yang, Y.-W.; Flood, A. H.; Fang, L.; Stoddart, J. F.; Weiss, P. S.; Huang, T. J. *ACS Nano* **2009**, *3*, 291–300.
- (4) (a) Deng, W.-Q.; Flood, A. H.; Stoddart, J. F.; Goddard, W. A. *J. Am. Chem. Soc.* **2005**, *127*, 15994–15995. (b) Ikeda, T.; Saha, S.; Arahamian, I.; Leung, K. F.; Williams, A.; Deng, W. Q.; Flood, A.; Goddard, W.; Stoddart, J. *Chem. Asian J.* **2007**, *2*, 76–93. (c) Ikeda, T.; Stoddart, J. F. *Sci. Technol. Adv. Mater.* **2008**, *9*.
- (5) (a) Jeppesen, J. O.; Nielsen, K. A.; Perkins, J.; Vignon, S. A.; Di Fabio, A.; Ballardini, R.; Gandolfi, M. T.; Venturi, M.; Balzani, V.; Becher, J.; Stoddart, J. F. *Chem.—Eur. J.* **2003**, *9*, 2982–3007. (b) Jeppesen, J. O.; Vignon, S. A.; Stoddart, J. F. *Chem.—Eur. J.* **2003**, *9*, 4611–4625. (c) Yamamoto, T.; Tseng, H.-R.; Stoddart, J. F.; Balzani, V.; Credi, A.; Marchioni, F.; Venturi, M. *Collect. Czech. Chem. Commun.* **2003**, *68*, 1488–1514. (d) Iijima, T.; Vignon, S. A.; Tseng, H.-R.; Jarrosson, T.; Sanders, J. K. M.; Marchioni, F.; Venturi, M.; Apostoli, E.; Balzani, V.; Stoddart, J. F. *Chem.—Eur. J.* **2004**, *10*, 6375–6392. (e) Zhang, W.; Dichtel, W. R.; Stieg, A. Z.; Benitez, D.; Gimzewski, J. K.; Heath, J. R.; Stoddart, J. F. *Proc. Natl. Acad. Sci. U.S.A.* **2008**, *105*, 6514–6519.
- (6) (a) Stanier, C. A.; Alderman, S. J.; Claridge, T. D. W.; Anderson, H. L. *Angew. Chem., Int. Ed.* **2002**, *41*, 1769–1772. (b) Qu, D.-H.; Wang, Q.-C.; Ma, X.; Tian, H. *Chem.—Eur. J.* **2005**, *11*, 5929–5937.
- (c) Durola, F.; Lux, J.; Sauvage, J.-P. *Chem.—Eur. J.* **2009**, *15*, 4124–4134. (d) Busseron, E.; Romuald, C.; Coutrot, F. *Chem.—Eur. J.* **2010**, *16*, 10062–10073. (e) Credi, A.; Venturi, M.; Balzani, V. *ChemPhysChem* **2010**, *11*, 3398–3403. (f) Davidson, G. J. E.; Sharma, S.; Loeb, S. J. *Angew. Chem., Int. Ed.* **2010**, *49*, 4938–4942. (g) Hsueh, S.-Y.; Kuo, C.-T.; Lu, T.-W.; Lai, C.-C.; Liu, Y.-H.; Hsu, H.-F.; Peng, S.-M.; Chen, C.-h.; Chiu, S.-H. *Angew. Chem., Int. Ed.* **2010**, *49*, 9170–9173. (h) Barin, G.; Coskun, A.; Friedman, D. C.; Olson, M. A.; Colvin, M. T.; Carmielli, R.; Dey, S. K.; Bozdemir, O. A.; Wasielewski, M. R.; Stoddart, J. F. *Chem.—Eur. J.* **2011**, *17*, 213–222. (i) Leontiev, A. V.; Jemmett, C. A.; Beer, P. D. *Chem.—Eur. J.* **2011**, *17*, 816–825. (j) Pierro, T.; Gaeta, C.; Talotta, C.; Casapullo, A.; Neri, P. *Org. Lett.* **2011**, *13*, 2650–2653.
- (7) Meijer, E. W. *Nature* **2011**, *469*, 23–25.
- (8) Fu, Z.-Q.; Du Bois, G. C.; Song, S. P.; Kulikovskaya, I.; Virgilio, L.; Rothstein, J. L.; Croce, C. M.; Weber, I. T.; Harrison, R. W. *Proc. Natl. Acad. Sci. U.S.A.* **1998**, *95*, 3413–3418.
- (9) Asakawa, M.; Dehaen, W.; L'Abbe, G.; Menzer, S.; Nouwen, J.; Raymo, F. M.; Stoddart, J. F.; Williams, D. J. *J. Org. Chem.* **1996**, *61*, 9591–9595.
- (10) (a) Houk, K. N.; Menzer, S.; Newton, S. P.; Raymo, F. M.; Stoddart, J. F.; Williams, D. J. *J. Am. Chem. Soc.* **1999**, *121*, 1479–1487. (b) Raymo, F. M.; Bartberger, M. D.; Houk, K. N.; Stoddart, J. F. *J. Am. Chem. Soc.* **2001**, *123*, 9264–9267. (c) Nygaard, S.; Hansen, C. N.; Jeppesen, J. O. *J. Org. Chem.* **2007**, *72*, 1617–1626.
- (11) (a) Bryce, M. R. *J. Mater. Chem.* **2000**, *10*, 589–598. (b) Segura, J. L.; Martín, N. *Angew. Chem., Int. Ed.* **2001**, *40*, 1372–1409. (c) Becher, J.; Jeppesen, J. O.; Nielsen, K. *Synth. Met.* **2003**, *133–134*, 309–315. (d) Jeppesen, J. O.; Nielsen, M. B.; Becher, J. *Chem. Rev.* **2004**, *104*, 5115–5132. (e) Otsubo, T. *Bull. Chem. Soc. Jpn.* **2004**, *77*, 43–58.
- (12) (a) Jeppesen, J. O.; Takimiya, K.; Jensen, F.; Becher, J. *Org. Lett.* **1999**, *1*, 1291–1294. (b) Jeppesen, J. O.; Takimiya, K.; Jensen, F.; Brimert, T.; Nielsen, K.; Thorup, N.; Becher, J. *J. Org. Chem.* **2000**, *65*, 5794–5805.
- (13) Marquis, D.; Desvergne, J.-P.; Bouas-Laurent, H. *J. Org. Chem.* **1995**, *60*, 7984–7996.
- (14) Gatto, V. J.; Arnold, K. A.; Viscariello, A. M.; Miller, S. R.; Morgan, C. R.; Gokel, G. W. *J. Org. Chem.* **1986**, *51*, 5373–5384.
- (15) Jia, C.; Zhang, D.; Xu, W.; Zhu, D. *Org. Lett.* **2001**, *3*, 1941–1944.
- (16) Svenstrup, N.; Rasmussen, K. M.; Hansen, T. K.; Becher, J. *Synthesis* **1994**, 809–812.
- (17) (a) Kopecky, K. R.; Yeung, M. Y. *Can. J. Chem.* **1988**, *66*, 374–376. (b) Plater, M. J.; Aiken, S.; Bourhill, G. *Tetrahedron* **2002**, *58*, 2405–2413.
- (18) Nielsen, M. B.; Jeppesen, J. O.; Lau, J.; Lomholt, C.; Damgaard, D.; Jacobsen, J. P.; Becher, J.; Stoddart, J. F. *J. Org. Chem.* **2001**, *66*, 3559–3563.
- (19) Nygaard, S.; Hansen, S. W.; Huffman, J. C.; Jensen, F.; Flood, A. H.; Jeppesen, J. O. *J. Am. Chem. Soc.* **2007**, *129*, 7354–7363.
- (20) Zhao, Y.; Truhlar, D. G. *J. Chem. Phys.* **2006**, *125*, 194101–1–194101–18.
- (21) *Jaguar, version 7.6*, Schrödinger, LLC, New York, NY, 2009.
- (22) (a) Benitez, D.; Tkatchouk, E.; Yoon, I.; Stoddart, J. F.; Goddard, W. A. *J. Am. Chem. Soc.* **2008**, *130*, 14928–14929. (b) Spruell, J. M.; Paxton, W. F.; Olsen, J.-C.; Benitez, D.; Tkatchouk, E.; Stern, C. L.; Trabolsi, A.; Friedman, D. C.; Goddard, W. A.; Stoddart, J. F. *J. Am. Chem. Soc.* **2009**, *131*, 11571–11580.
- (23) (a) Philp, D.; Slawin, A. M. Z.; Spencer, N.; Stoddart, J. F.; Williams, D. J. *J. Chem. Soc., Chem. Commun.* **1991**, 1584–1586. (b) Asakawa, M.; Ashton, P. R.; Balzani, V.; Credi, A.; Hamers, C.; Mattersteig, G.; Montalti, M.; Shipway, A. N.; Spencer, N.; Stoddart, J. F.; Tolley, M. S.; Venturi, M.; White, A. J. P.; Williams, D. J. *Angew. Chem., Int. Ed.* **1998**, *37*, 333–337.
- (24) (a) Nygaard, S.; Liu, Y.; Stein, P. C.; Flood, A. H.; Jeppesen, J. O. *Adv. Funct. Mater.* **2007**, *17*, 751–762. (b) Tseng, H. R.; Vignon, S. A.; Celestre, P. C.; Perkins, J.; Jeppesen, J. O.; Di Fabio, A.; Ballardini,

R.; Gandolfi, M. T.; Venturi, M.; Balzani, V.; Stoddart, J. F. *Chem.—Eur. J.* **2004**, *10*, 155–172.

(25) A comparison of oxidation potentials of MPTTF compounds with and without thio substituents on one of the dithiole positions can be found in: ref 10c. It is assumed that the same trend will be applicable to TTF compounds with and without thio substituents on one of the dithiole positions.

(26) To the best of our knowledge, no successful experiments describing NOE effects for complexes based on TTF derivatives and CBPQT<sup>4+</sup> have been reported. However, NOE effects have been reported for complexes based on CBPQT<sup>4+</sup> and other electron donors, see. (a) Liu, Y.; Flood, A. H.; Moskowitz, R. M.; Stoddart, J. F. *Chem.—Eur. J.* **2005**, *11*, 369–385. (b) Caldwell, S. T.; Cooke, G.; Cooper, A.; Nutley, M.; Rabani, G.; Rotello, V.; Smith, B. O.; Woisel, P. *Chem. Commun.* **2008**, 2650–2652. (c) Ikeda, T.; Higuchi, M.; Kurth, D. G. *Chem.—Eur. J.* **2009**, *15*, 4906–4913. (d) Cao, J.; Guo, J.-B.; Li, P.-F.; Chen, C.-F. *J. Org. Chem.* **2011**, *76*, 1644–1652.

(27) The equilibrium constant  $K_{\text{eq}}$  for the equilibrium between the unfolded 2° structure and the folded 3° structure was calculated using the relationship  $K_{\text{eq}} = \exp(\Delta G/RT)$ , where  $R$  is the gas constant and  $T$  is the absolute temperature.